GEOLOGY | THE GEOLOGICAL SOCIETY OF AMERICA®

https://doi.org/10.1130/G50615.1

Manuscript received 30 May 2022
Revised manuscript received 26 July 2022
Manuscript accepted 27 September 2022

Published online 3 January 2023

© 2022 The Authors. Gold Open Access: This paper is published under the terms of the CC-BY license.

Phanerozoic cratonization by plume welding

Xi Xu[1,2,3], Hanlin Chen[2]*, Andrew V. Zuza[4], An Yin[3], Peng Yu[5], Xiubin Lin[2], Chongjin Zhao[5], Juncheng Luo[6], Shufeng Yang[2] and Baodi Wang[1]

[1]China Aero Geophysical Survey and Remote Sensing Center for Natural Resources, China Geological Survey, Beijing 100083, China
[2]School of Earth Sciences, Zhejiang University, Hangzhou 310027, China
[3]Department of Earth, Planetary, and Space Sciences, University of California, Los Angeles, California 90925, USA
[4]Nevada Bureau of Mines and Geology, University of Nevada, Reno, Nevada 89557, USA
[5]School of Ocean and Earth Science, Tongji University, Shanghai 200092, China
[6]Tarim Oilfield Company, PetroChina, Korla 841000, China

ABSTRACT

Deformation-resistant cratons comprise >60% of the continental landmass on Earth. Because they were formed mostly in the Archean to Mesoproterozoic, it remains unclear if cratonization was a process unique to early Earth. We address this question by presenting an integrated geological-geophysical data set from the Tarim region of central Asia. This data set shows that the Tarim region was a deformable domain from the Proterozoic to early Paleozoic, but deformation ceased after the emplacement of a Permian plume despite the fact that deformation continued to the north and south due to the closure of the Paleo-Asian and Tethyan Oceans. We interpret this spatiotemporal correlation to indicate plume-driven welding of the earlier deformable continents and the formation of Tarim's stable cratonic lithosphere. Our work highlights the Phanerozoic plume-driven cratonization process and implies that mantle plumes may have significantly contributed to the development of cratons on early Earth.

INTRODUCTION

Cratons are characterized by a > 150-km-thick lithospheric mantle root, resistance to deformation imposed by plate-boundary forces, and dominantly Archean–Mesoproterozoic ages (e.g., Bedle et al., 2021; Pearson et al., 2021). It remains an open question as to whether the development of a strong cratonic keel and cratonization were uniquely early Earth processes, possibly aided by higher mantle potential temperatures (Herzberg and Rudnick, 2012; Gerya et al., 2015) and repeated orogenesis (McKenzie and Priestley, 2016; Pearson et al., 2021). Well-documented examples of the Mesozoic destruction of Archean cratons by plate-tectonic (e.g., North China craton; Menzies et al., 1993) or plume-driven (e.g., Africa craton; Hu et al., 2018; Celli et al., 2020) processes suggest a dynamic evolution of cratonic lithosphere throughout Earth history (Bedle et al., 2021).

The role of mantle plumes in the evolution of the cratonic mantle lithosphere is contentious. Mantle plumes may (re)grow the continental mantle keel via basal accretion (Lee et al., 2011; Liu et al., 2021) or destroy the mantle root by convective removal or thermally induced delamination (Hu et al., 2018; Celli et al., 2020). Plume-lithosphere interactions may drive mantle melt depletion to generate thick, buoyant continental mantle capable of resisting future continental deformation (Xu et al., 2021). If plume processes can build stable cratonic mantle keels (>150 km) via mass and heat exchange between the crust and mantle (Jordan, 1978; Pearson et al., 2021), cratonization should have occurred throughout Earth history. Furthermore, the probability of craton generation in a particular geologic period should depend on the frequency and spatial abundance of mantle plumes.

The Tarim region of central Asia (Fig. 1A) exhibits a unique geologic history best explained by Permian plume-induced welding of Precambrian lithosphere. We detail this mechanism by presenting new magnetic data, three-dimensional (3-D) inverse modeling results, and high-resolution seismic profiles that elucidate the extent and consequence of the plume emplacement below the Tarim region. We demonstrate that Tarim's lithospheric thickness increased and deformation ceased after the plume impingement.

GEOLOGIC SETTING

The Tarim domain contains the North and South Tarim terranes, with Precambrian basement rocks separated by a Neoproterozoic suture that was reactivated in the early Paleozoic (Figs. 1B and 1C; Fig. S1 in the Supplemental Material[1]; Guo et al., 2005; Zuza and Yin, 2017; Zhao et al., 2021). Despite earlier Neoproterozoic–early Paleozoic deformation, the region has remained undeformed since the Carboniferous, as indicated by a regional Carboniferous unconformity over deformed early Paleozoic strata (Guo et al., 2005). The post-Carboniferous stability of the Tarim region could be attributed to the lack of plate boundary–induced deformation, but the closure of the Tethyan oceans in the Mesozoic should have renewed deformation across Tarim since the late Permian, which is not observed (e.g., Yin and Harrison, 2000). The transition from the earlier deformable to the later nondeformable state correlates with the emplacement of a mantle plume at ca. 300–270 Ma, which may have strengthened Tarim's mantle lithosphere (Xu et al., 2021).

The Tarim Permian plume activity generated a large igneous province (LIP; > 250,000 km^2) and (ultra)mafic to felsic intrusions (Fig. 1; Xu et al., 2014). Initial plume impingement occurred beneath western Tarim at ca. 300 Ma, followed by crustal doming uplift/erosion, regional unconformities (Li et al., 2014; Xu et al., 2014), high-temperature (>800 °C) anatexis, juvenile rhyolite volcanism, and protracted mantle-derived intrusions (Xu et al., 2014).

*E-mail: hlchen@zju.edu.cn

[1]Supplemental Material. Geophysical compilation and details for magnetic inversion, lithospheric structure, and seismic-based interpretation. Please visit https://doi.org/10.1130/GEOL.S.21644663 to access the supplemental material and contact editing@geosociety.org with any questions.

CITATION: Xu, X., et al., 2023, Phanerozoic cratonization by plume welding: Geology, v. XX, p. , https://doi.org/10.1130/G50615.1

Downloaded from http://pubs.geoscienceworld.org/gsa/geology/article-pdf/doi/10.1130/G50615.1/5761921/g50615.pdf
by guest

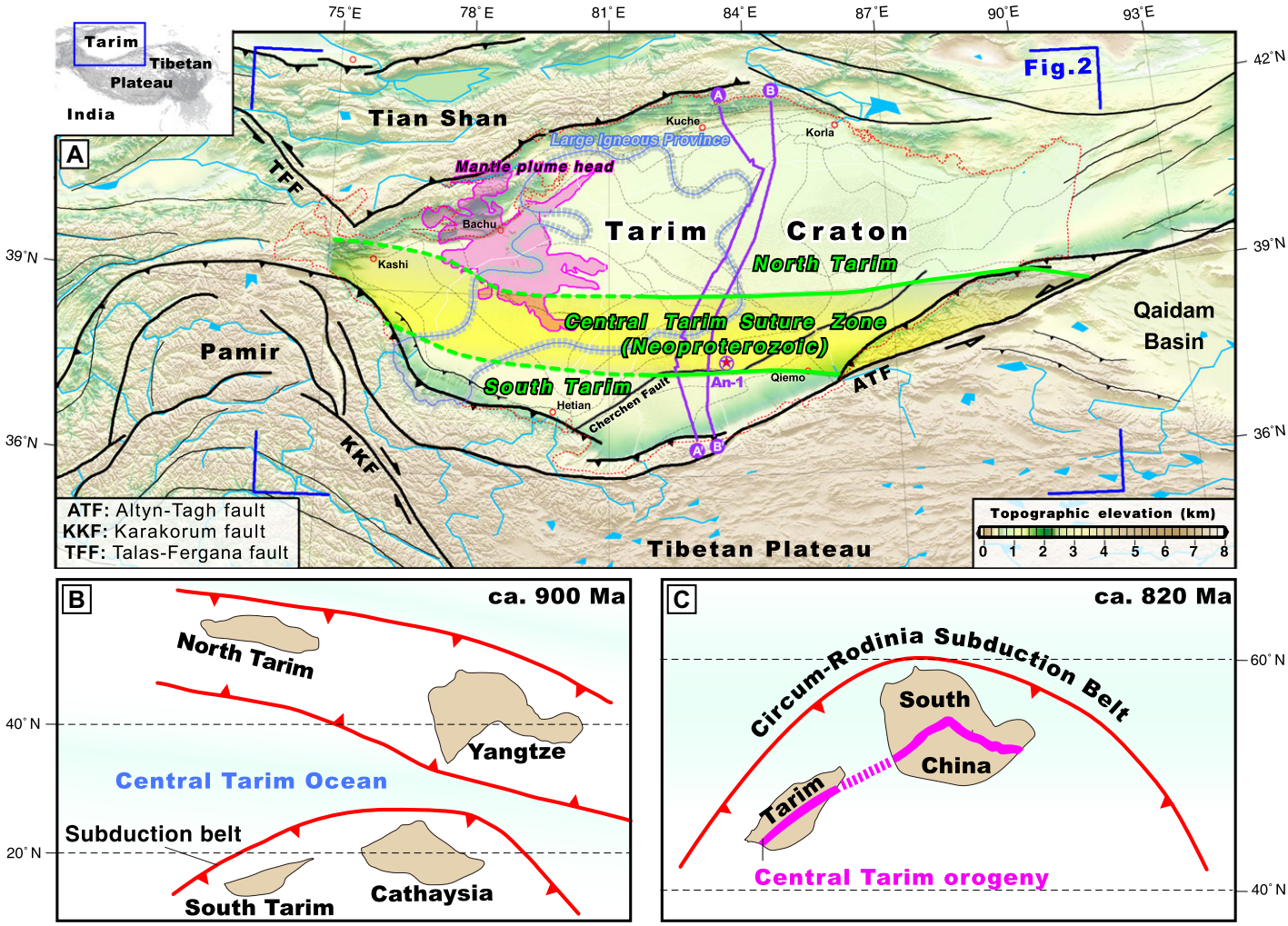

Figure 1. (A) Tectonic map of the Tarim domain and its surrounding regions in central Asia. Profiles A-A′ and B-B′ are industry seismic sections. Geometry and location of the mantle plume head are from Xu et al. (2021). Location of the Central Tarim suture zone (CTSZ) is from Zhao et al. (2021). Borehole An-1 is labeled by the violet star. (B,C) Paleogeographic Neoproterozoic reconstructions (Zhao et al., 2021) of Tarim at ca. 900 Ma (B) and ca. 820 Ma (C).

NEW GEOPHYSICAL CONSTRAINTS

Extensive Cenozoic sedimentary cover makes it difficult to estimate the extent of the region affected by the Permian plume. To overcome this issue, we used aeromagnetic data that are sensitive to iron-rich mafic rocks (Grant, 1985; Frost and Shive, 1986; Saltus et al., 1999). We determined the distribution of magnetic bodies across the Tarim region by performing a 3-D regularization inversion of the aeromagnetic data (Figs. S2 and S3 and the Supplemental text ; e.g., Hu et al., 2019). The model consisted of 130 × 74 × 50 grid cells at a resolution of 10 × 10 × 1 km. Our results reveal a ring-like pattern of magnetic anomalies with increasing magnitudes from the upper (~10 km) to lower (~45 km) crust (Figs. S3B and S4). A circular magnetic low was observed in the center of the ring-like structure (H in Fig. 2; Fig. S4), and its diameter decreases from ~150 to ~25 km from depths of 45 to 10 km, respectively. A zone of 170 × 45 km west-trending, highly magnetic anomalies (HMAs) at depths of ~25–40 km traverses across most of the Tarim domain (Fig. S4); the same zone also intersects the ring-like anomaly (Fig. 2; Fig. S4). Two northeast-trending, mid- to lower-crustal anomalies (T1 and T2-T3 in Fig. 2) are transcrustal features cutting upward from 50 to 25 km (Fig. S4). An isolated anomaly (T4 in Fig. 2) in westernmost Tarim occurs at depths of 30–45 km, with an increasing magnetic intensity and extent with depth (Fig. S4), whereas an anomaly in northernmost Tarim (M in Fig. 2; Fig. S4) is less extensive with depth.

We interpreted two north-south–oriented seismic profiles (Fig. 3). They both traversed the Central Tarim suture zone and imaged to ~15 km depth, with age assignments from industry drill core (Fig. S5). A regional unconformity is present at the base of Carboniferous strata at ~6 km depth across the basin (Fig. 3). Above the unconformity, flat-lying reflectors suggest Mesozoic–Cenozoic strata are largely undeformed, consistent with the present-day Tarim region's low relief. Toward its southern end, post-Carboniferous reflectors are sharply truncated against the Cenozoic left-slip Cherchen fault (Fig. 3). South of this structure, reflectors that represent the basal Carboniferous unconformity are folded and truncated, suggesting relatively strong deformation in this southern domain. Below the Carboniferous unconformity, early Paleozoic strata and Proterozoic basement are penetratively folded and faulted with series of thrust faults, with the highest frequency of deformation correlating with the suture zone (Fig. 3).

DISCUSSION

The prominent high-amplitude, long-wavelength, crust-scale magnetic anomalies observed in this study are interpreted as thick mafic intrusions (Figs. S2B and S4; Grant, 1985; Frost and Shive, 1986; Saltus et al., 1999). The northeast-trending transcrustal anomalies (T1 and T2-T3 in Fig. 3) cut across the suture zone and the early Paleozoic orogenic belt in central Tarim (Fig. 1), requiring their formation to postdate both tectonic features. We interpret these anomalies to have formed by the impingement of the Perm-

Downloaded from http://pubs.geoscienceworld.org/gsa/geology/article-pdf/doi/10.1130/G50615.1/5761921/g50615.pdf
by guest

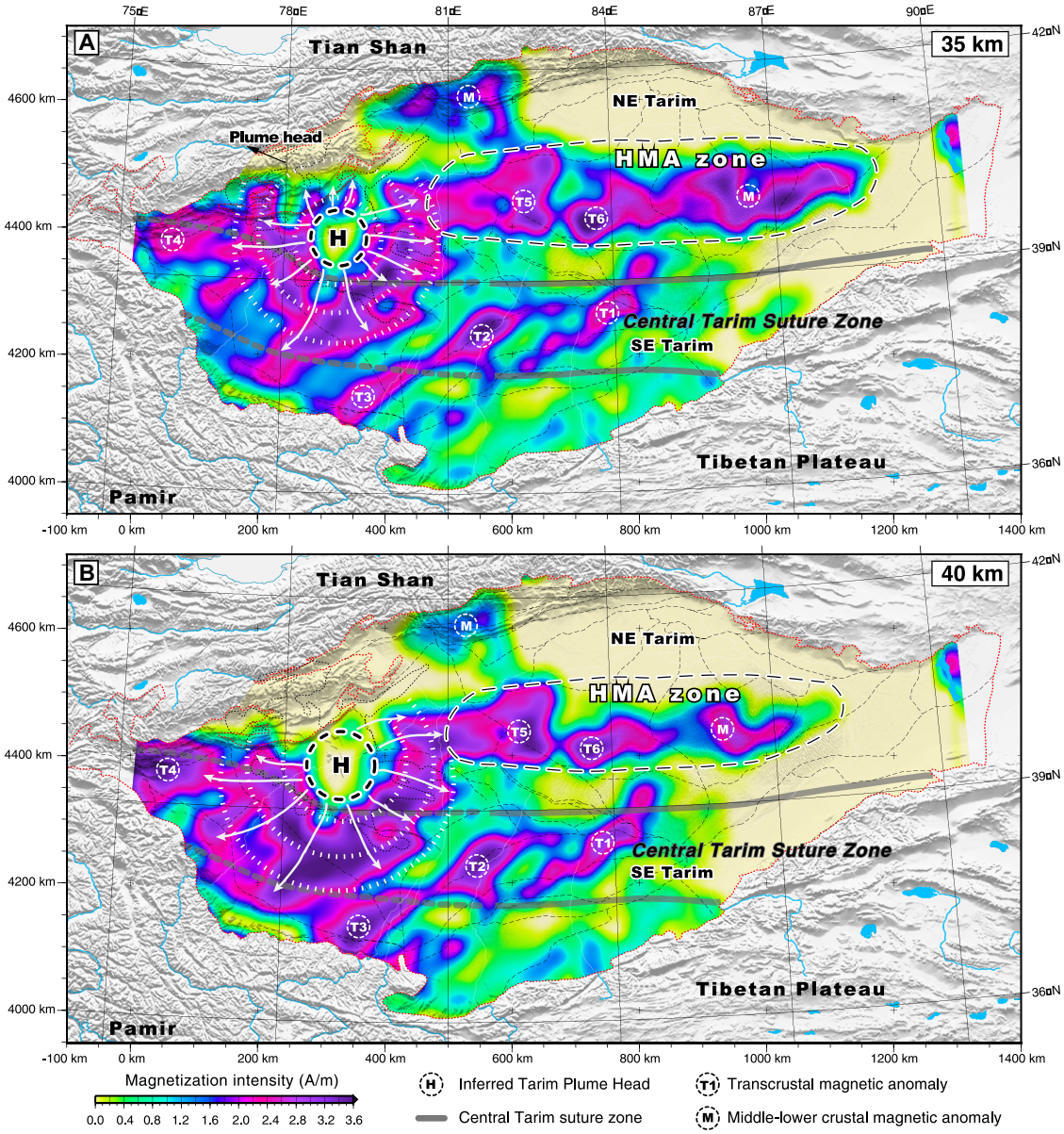

Figure 2. Horizontal slices of the inverted magnetization intensity model at depths of 35 km (A) and 45 km (B). HMA—highly magnetic anomaly. White arrows and dotted circular curves show the interpreted radial patterns of mid- to lower-crust mafic intrusions related to the Permian plume head (H).

ian plume because its emplacement was the only regional Phanerozoic igneous activity in this area (Xu et al., 2014). We suggest the ring-like magnetic patterns represent mafic intrusions emanating from the plume head (Fig. 4). The ring-like anomaly truncates the HMA zone, thus requiring the zone to predate the Permian. The HMA zone may represent an Archean nucleus with characteristic long-wavelength magnetic highs, similar to HMAs distributed across other cratons within China (e.g., the Ordos and Sichuan cratons; Fig. S6) and globally (Fig. S7; Maus et al., 2009).

Early Paleozoic reactivation of the Neoproterozoic suture between North and South Tarim (Fig. 1) led to deformation of early Paleozoic and older rocks, which were covered by Carboniferous-to-younger strata with an angular unconformity (Fig. 3). Boreholes show subtle domal uplifting and regional unconformities that correspond to the initial ca. 300 Ma impingement of the Tarim mantle plume (Li et al., 2014), but Mesozoic–Cenozoic strata are mostly flat lying, demonstrating negligible deformation since the late Paleozoic. The profiles across the central Tarim Basin reveal deformational patterns before and after the Carboniferous (Fig. 3), including the correspondence between strain and crustal composition interpreted from the magnetic inversion (Fig. 2). Parts of the profiles interpreted to be underlain by large mafic bodies show no post-Carboniferous strain, whereas those in the southeast without magnetically imaged mafic bodies experienced some deformation (Fig. 2). The absence of post-Permian deformation persists today, despite the closure of the Paleo-Asian and Tethyan ocean systems, which resulted in pervasive Mesozoic–Cenozoic deformation to the north and south (Windley et al., 1990; Yin and Harrison, 2000). These observations require the Tarim region to have become a deformation-resistant craton-like continent since Permian plume emplacement.

In summary, voluminous mafic intrusions overprint and postdate Neoproterozoic suture-zone structures. The observed magnetic features radiating outward from the center of the plume head are absent in the southeast Tarim domain, which was more strongly deformed than central-western Tarim (Fig. 2). These observations suggest that the mid- to lower-crust mafic intrusions derived from the Permian plume stitched and welded the suture zone, making the Tarim region stronger than its surrounding areas. The distribution of crustal mafic bodies across Tarim overlaps the regions with higher crustal velocity (Fig. S8; Bao et al., 2015) and density (Fig. S9A; Deng et al., 2017), which supports our interpretations.

Crustal enrichment of mafic materials is compositionally related to the extraction and depletion of the underlying mantle (Jordan, 1978), which could generate a cratonic mantle keel (Jordan, 1978; Pearson et al., 2021). We interpret that the Permian mantle plume may

Downloaded from http://pubs.geoscienceworld.org/gsa/geology/article-pdf/doi/10.1130/G50615.1/5761921/g50615.pdf
by guest

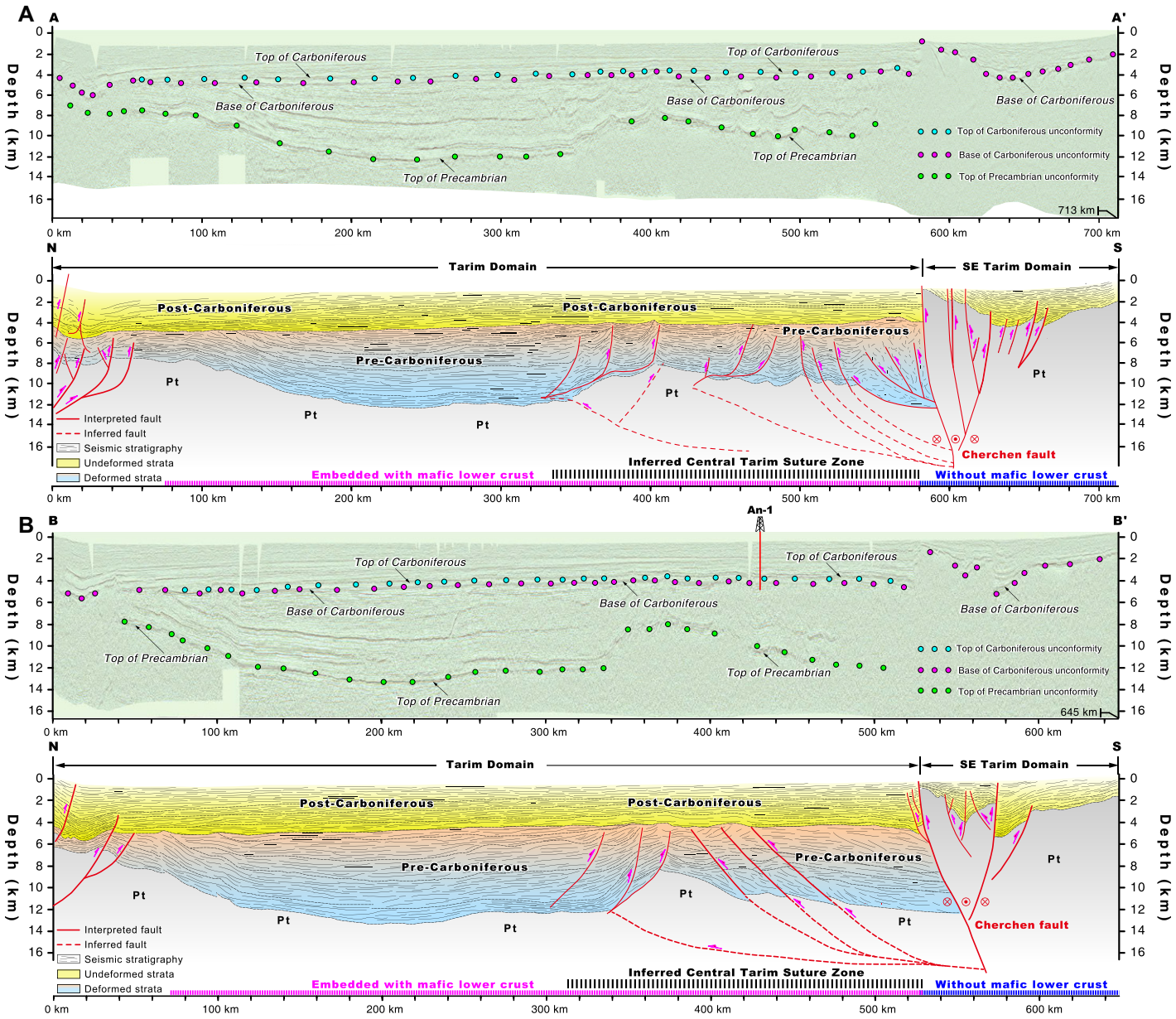

Figure 3. Uninterpreted and interpreted seismic sections A-A′ and B-B′ (purple lines in Figure 1). Pink and blue dot lines indicate our interpretations of the middle-lower crust embedded with and without significant mafic intrusions, respectively. Borehole An-1 (Fig. S5 [see footnote 1]) is projected onto seismic profile B-B′ to constrain reflector interpretations. Pt—Proterozoic basement.

have initially impinged upon the relatively thin, metasomatized lithosphere along the Tarim suture zone, potentially causing further local thinning via thermal erosion, which thus allowed the generation of a large volume of melts and crustal magmatism by ca. 290 Ma (Fig. 4A; Xu et al., 2014). Assimilation and fractional crystallization of the melts may have, in turn, led to the formation of the central magma conduit of the plume composed mostly of high–Nb-Ta rhyolites (Fig. 2; Xu et al., 2014). The plume-derived mantle melts modified the crust via lower-crust underplating (Xu and He, 2007; Chen et al., 2015) and the emplacement of mafic intrusions across the entire crust. This heat and mass transfer process built a dehydrated, depleted, and thickened mantle root that coherently welded the sutured Tarim lithosphere (Fig. 4A). The patchwork, relatively thin Permian lithosphere (<150 km; Xu et al., 2014) was subsequently thickened to >200 km today (Xu et al., 2002).

The region most modified by the mantle plume, as tracked via magnetic signals, corresponds to an inferred mantle keel with high velocity, reduced density, and high resistivity (Figs. S8 and S9B; Bao et al., 2015; Deng et al., 2017; Zhang et al., 2020). In our model, plume-derived, melt-depleted mantle residue accreted to the base of the Tarim lithosphere to form a structurally intact cratonic lithosphere (Fig. 4B), which explains the present-day >200 km mantle root (Xu et al., 2002; Bao et al., 2015) and Cenozoic tectonic quiescence (Guo et al., 2005).

Although geophysical observations suggest lithospheric modification correlative with the plume-head location (Figs. S8 and S9B), eastern Tarim shows more variability of relative lithospheric density and resistivity (Deng et al., 2017; Zhang et al., 2020). These differences likely reflect heterogeneous inherited mantle lithosphere characteristics from the Precambrian continental terranes, early Paleozoic lithospheric thickening during orogeny (McKenzie and Priestley, 2016; Pearson et al., 2021), and spatially variable plume melt depletion (Liu et al., 2021). The Precambrian North and South Tarim terranes have Archean nuclei, consistent with our HMA interpretations, which may have consisted of initial, variably thick continental mantle. The Permian plume would have impinged, welded,

Downloaded from http://pubs.geoscienceworld.org/gsa/geology/article-pdf/doi/10.1130/G50615.1/5761921/g50615.pdf
by guest

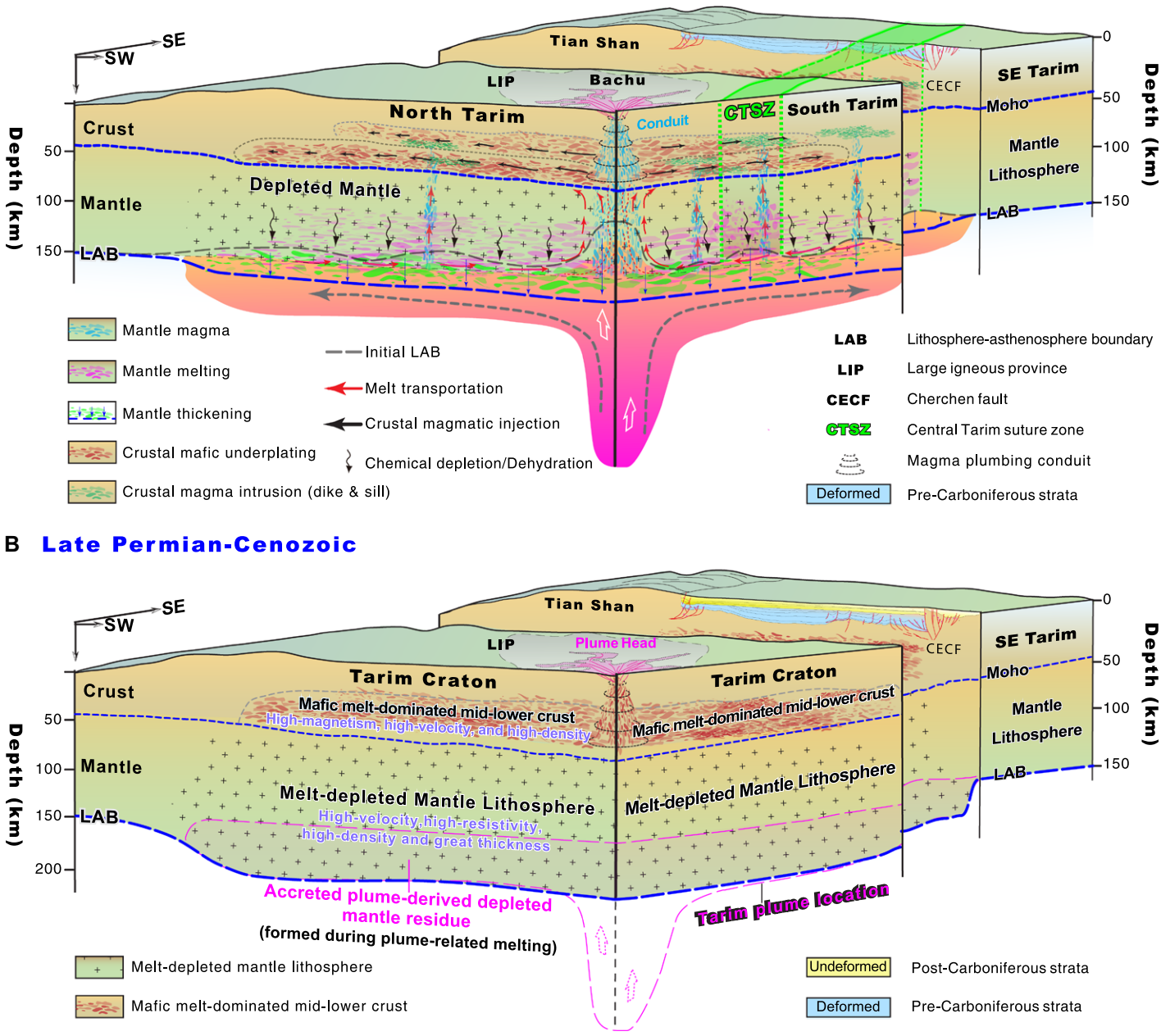

Figure 4. Conceptual model of a plume welding the continental lithosphere of the merged North and South Tarim domain. (A) Late Carboniferous–early Permian. The plume impinged on the sutured Tarim lithosphere, associated with large igneous province (LIP) volcanism and mafic intrusions in the mid- to lower crust. Plume-lithosphere interaction modified the lithospheric mantle via melting, depletion, and thickening, coupled with pervasive mid- to lower-crustal intrusions to construct coherent cratonic lithosphere across the suture zone. (B) Late Permian–Cenozoic. Plume-driven, melt-depleted mantle residue accreted to the lithospheric mantle and completely welded the lithospheric mantle of the integrated Tarim craton.

and cratonized this initially heterogeneous continental mantle (Fig. 4; Pearson et al., 2021).

Although mantle plumes may erode mantle lithosphere and even drive their delamination (Hu et al., 2018; Celli et al., 2020), plume impingement can be important for building (Lee et al., 2011) or healing (Liu et al., 2021) a strong mantle root. Plume-driven cratonization can strengthen preexisting weaknesses in the lithosphere, such as suture zones (Heron et al., 2016). Conversely, the other main suture zones in Tibet were strongly deformed by Cenozoic orogeny (Yin and Harrison, 2000; Zuza et al., 2018). Mountain building is an alternative mechanism to thicken the mantle lithosphere (McKenzie and Priestley, 2016) and potentially generate a cratonic keel (Pearson et al., 2021). However, we can rule out the possibility that Tarim was cratonized solely by early Paleozoic orogeny because the coeval fold-and-thrust belt outside the plume-impacted region was reactivated by Cenozoic deformation in northern Tibet (Zuza et al., 2018). Thus, the protracted history of early Paleozoic orogeny and lithospheric thickening followed by plume impingement and welding possibly represents a protracted cycle of cratonization (Pearson et al., 2021).

Given billions of years of plume activity in Earth history (Condie, 2001), this documented process may have been important for developing cratonic mantle throughout Earth history. Plume-related continental mantle development may be associated with a crustal record consisting of iron-rich mid- to lower crust that

Downloaded from http://pubs.geoscienceworld.org/gsa/geology/article-pdf/doi/10.1130/G50615.1/5761921/g50615.pdf
by guest

is detectable via magnetic imaging. Many cratons nested within global continents have high-amplitude, long-wavelength magnetic highs that may reflect voluminous mafic material in the mid- to lower crust (Fig. S7; Frost and Shive, 1986; Maus et al., 2009), which was ultimately extracted from the melt-depleted mantle as originally envisioned by Jordan (1978).

Higher mantle potential temperatures in early Earth require more rigorous, frequent, and regionally extensive plume activities, which may have affected the evolution of the continental lithosphere (Herzberg and Rudnick, 2012; Gerya et al., 2015; Bedle et al., 2021). In contrast, reduced Phanerozoic plume activity (Tomlinson and Condie, 2001) means that cratonization, as suggested by the Phanerozoic evolution of the Tarim lithosphere, was rare. Taken together, the plume-dominated first half of Earth's history would have favored the formation of stable continental regions that we refer to today as cratons.

ACKNOWLEDGMENTS

We thank Xuewei Bao for sharing the seismic velocity data. This research was supported by the Second Tibetan Plateau Scientific Expedition and Research (grant 2019QZKK00708), the National Natural Science Foundation of China (grants 41902202, 42072233 and 41720104003), the U.S. National Science Foundation (grant 1914501), the China Postdoctoral Science Foundation (grant 2019M652062), and the Geological Survey Project of China (grants DD20211396 and DD20221715). Reviews by Yigang Xu, Jiawei Zuo, Jingao Liu, and three anonymous reviewers improved this paper. We appreciate the manuscript handling by editor R. Strachan.

REFERENCES CITED

Bao, X.W., Song, X.D., and Li, J.T., 2015, High-resolution lithospheric structure beneath Mainland China from ambient noise and earthquake surface-wave tomography: Earth and Planetary Science Letters, v. 417, p. 132–141, https://doi.org/10.1016/j.epsl.2015.02.024.

Bedle, H., Cooper, C.M., and Frost, C.D., 2021, Nature versus nurture: Preservation and destruction of Archean cratons: Tectonics, v. 40, https://doi.org/10.1029/2021TC006714.

Celli, N.L., Lebedev, S., Schaeffer, A.J., and Gaina, C., 2020, African cratonic lithosphere carved by mantle plumes: Nature Communications, v. 11, p. 1–10, https://doi.org/10.1038/s41467-019-13871-2.

Chen, Y., Xu, Y., Xu, T., Si, S., Liang, X., Tian, X., Deng, Y., Chen, L., Wang, P., Xu, Y., and Lan, H., 2015, Magmatic underplating and crustal growth in the Emeishan large igneous province, SW China, revealed by a passive seismic experiment: Earth and Planetary Science Letters, v. 432, p. 103–114, https://doi.org/10.1016/j.epsl.2015.09.048.

Condie, K.C., 2001, Mantle Plumes and Their Record in Earth History: New York, Cambridge University Press, 303 p., https://doi.org/10.1017/CBO9780511810589.

Deng, Y., Levandowski, W., and Kusky, T., 2017, Lithospheric density structure beneath the Tarim basin and surroundings, northwestern China, from the joint inversion of gravity and topography: Earth and Planetary Science Letters, v. 460, p. 244–254, https://doi.org/10.1016/j.epsl.2016.10.051.

Frost, B.R., and Shive, P.N., 1986, Magnetic mineralogy of the lower continental crust: Journal of Geophysical Research–Solid Earth, v. 91, p. 6513–6521, https://doi.org/10.1029/JB091iB06p06513.

Gerya, T.V., Stern, R.J., Baes, M., Sobolev, S.V., and Whattam, S.A., 2015, Plate tectonics on the Earth triggered by plume-induced subduction initiation: Nature, v. 527, p. 221–225, https://doi.org/10.1038/nature15752.

Grant, F.S., 1985, Aeromagnetics, geology and ore environments: I. Magnetite in igneous, sedimentary and metamorphic rocks: An overview: Geoexploration, v. 23, p. 303–333, https://doi.org/10.1016/0016-7142(85)90001-8.

Guo, Z.J., Yin, A., Robinson, A., and Jia, C.Z., 2005, Geochronology and geochemistry of deep-drill-core samples from the basement of the central Tarim basin: Journal of Asian Earth Sciences, v. 25, p. 45–56, https://doi.org/10.1016/j.jseaes.2004.01.016.

Heron, P.J., Pysklywec, R.N., and Stephenson, R., 2016, Lasting mantle scars lead to perennial plate tectonics: Nature Communications, v. 7, p. 1–7, https://doi.org/10.1038/ncomms11834.

Herzberg, C., and Rudnick, R., 2012, Formation of cratonic lithosphere: An integrated thermal and petrological model: Lithos, v. 149, p. 4–15, https://doi.org/10.1016/j.lithos.2012.01.010.

Hu, J., Liu, L., Faccenda, M., Zhou, Q., Fischer, K.M., Marshak, S., and Lundstrom, C., 2018, Modification of the Western Gondwana craton by plume-lithosphere interaction: Nature Geoscience, v. 11, p. 203–210, https://doi.org/10.1038/s41561-018-0064-1.

Hu, M., Yu, P., Rao, C., Zhao, C., and Zhang, L., 2019, 3D sharp-boundary inversion of potential-field data with an adjustable exponential stabilizing functional: Geophysics, v. 84, p. 1–15, https://doi.org/10.1190/geo2018-0132.1.

Jordan, T.H., 1978, Composition and development of the continental tectosphere: Nature, v. 274, p. 544–548, https://doi.org/10.1038/274544a0.

Lee, C.T.A., Luffi, P., and Chin, E.J., 2011, Building and destroying continent mantle: Annual Review of Earth and Planetary Sciences, v. 39, p. 59–90, https://doi.org/10.1146/annurev-earth-040610-133505.

Li, D., Yang, S., Chen, H., Cheng, X., Li, K., Jin, X., Li, Z., Li, Y., and Zou, S., 2014, Late Carboniferous crustal uplift of the Tarim plate and its constraints on the evolution of the Early Permian Tarim Large Igneous Province: Lithos, v. 204, p. 36–46, https://doi.org/10.1016/j.lithos.2014.05.023.

Liu, J.G., Pearson, D.G., Wang, L.H., Mather, K.A., Kjarsgaard, B.A., Schaeffer, A.J., Irvine, G.J., Kopylova, M.G., and Armstrong, J.P., 2021, Plume-driven recratonization of deep continental lithospheric mantle: Nature, v. 592, p. 732–736, https://doi.org/10.1038/s41586-021-03395-5.

Maus, S., Barckhausen, U., Berkenbosch, H., Bournas, N., Brozena, J., Childers, V., Dostaler, F., Fairhead, J.D., Finn, C., and Von Frese, R., 2009, EMAG2: A 2-arc min resolution Earth magnetic anomaly grid compiled from satellite, airborne, and marine magnetic measurements: Geochemistry Geophysics Geosystems, v. 10, Q08005, https://doi.org/10.1029/2009GC002471.

McKenzie, D., and Priestley, K., 2016, Speculations on the formation of cratons and cratonic basins: Earth and Planetary Science Letters, v. 435, p. 94–104, https://doi.org/10.1016/j.epsl.2015.12.010.

Menzies, M.A., Fan, W.M., and Zhang, M., 1993, Paleozoic and Cenozoic lithoprobe and the loss of >120 km of Archean lithosphere, Sino-Korean craton, China, *in* Prichard, H.M., et al., eds., Magmatic Processes and Plate Tectonics: Geological Society, London, Special Publication 76, p. 71–81, https://doi.org/10.1144/GSL.SP.1993.076.01.04.

Pearson, D.G., Scott, J.M., Liu, J., Schaeffer, A., Wang, L.H., van Hunen, J., Szilas, K., Chacko, T., and Kelemen, P.B., 2021, Deep continental roots and cratons: Nature, v. 596, p. 199–210, https://doi.org/10.1038/s41586-021-03600-5.

Saltus, R.W., Hudson, T.L., and Connard, G.G., 1999, A new magnetic view of Alaska: GSA Today, v. 9, no. 3, p. 1–6.

Tomlinson, K.Y., and Condie, K.C., 2001, Archean mantle plumes: Evidence from greenstone belt geochemistry, *in* Ernst, R.E., and Buchan, K.L., eds., Mantle Plumes: Their Identification Through Time: Geological Society of America Special Paper 352, p. 341–357, https://doi.org/10.1130/0-8137-2352-3.341.

Windley, B.F., Allen, M.B., Zhang, C., Zhao, Z.Y., and Wang, G.R., 1990, Paleozoic accretion and Cenozoic redeformation of the Chinese Tien Shan range, central Asia: Geology, v. 18, p. 128–131, https://doi.org/10.1130/0091-7613(1990)018<0128:PAACRO>2.3.CO;2.

Xu, X., Zuza, A.V., Yin, A., Lin, X., Chen, H., and Yang, S., 2021, Permian plume-strengthened Tarim lithosphere controls the Cenozoic deformation pattern of the Himalayan-Tibetan orogen: Geology, v. 49, p. 96–100, https://doi.org/10.1130/G47961.1.

Xu, Y., Liu, F., Liu, J., and Chen, H., 2002, Crust and upper mantle structure beneath western China from P wave travel time tomography: Journal of Geophysical Research–Solid Earth, v. 107, 2220, https://doi.org/10.1029/2001JB000402.

Xu, Y.G., and He, B., 2007, Thick and high velocity crust in Emeishan large igneous province, SW China: Evidence for crustal growth by magmatic underplating or intraplating, *in* Foulger, G.R., and Jurdy, D.M., eds., Plates, Plumes, and Planetary Processes: Geological Society of America Special Paper 430, p. 841–858, https://doi.org/10.1130/2007.2430(39).

Xu, Y.G., Wei, X., Luo, Z., Liu, H., and Cao, J., 2014, The early Permian Tarim large igneous province: Main characteristics and a plume incubation model: Lithos, v. 204, p. 20–35, https://doi.org/10.1016/j.lithos.2014.02.015.

Yin, A., and Harrison, T.M., 2000, Geologic evolution of the Himalayan-Tibetan orogen: Annual Review of Earth and Planetary Sciences, v. 28, p. 211–280, https://doi.org/10.1146/annurev.earth.28.1.211.

Zhang, L.L., Zhao, C.J., Yu, P., Xiang, Y., Peng, X., Koyama, T., and Yang, W., 2020, The electrical conductivity structure of the Tarim basin in NW China as revealed by three-dimensional magnetotelluric inversion: Journal of Asian Earth Sciences, v. 187, https://doi.org/10.1016/j.jseaes.2019.104093.

Zhao, P., He, J., Deng, C., Chen, Y., and Mitchell, R.N., 2021, Early Neoproterozoic (870–820 Ma) amalgamation of the Tarim craton (northwestern China) and the final assembly of Rodinia: Geology, v. 49, p. 1277–1282, https://doi.org/10.1130/G48837.1.

Zuza, A.V., and Yin, A., 2017, Balkatach hypothesis: A new model for the evolution of the Pacific, Tethyan, and Paleo-Asian oceanic domains: Geosphere, v. 13, p. 1664–1712, https://doi.org/10.1130/GES01463.1.

Zuza, A.V., Wu, C., Reith, R.C., Yin, A., Li, J., Zhang, J., Zhang, Y., Wu, L., and Liu, W., 2018, Tectonic evolution of the Qilian Shan: An early Paleozoic orogen reactivated in the Cenozoic: Geological Society of America Bulletin, v. 130, p. 881–925, https://doi.org/10.1130/B31721.1.

Printed in USA

Downloaded from http://pubs.geoscienceworld.org/gsa/geology/article-pdf/doi/10.1130/G50615.1/5761921/g50615.pdf
by guest